Michal Kurka, Karel Palka, Jiri Jancalek, Stanislav Slang, Jakub Houdek, Miroslav Vlcek (2023). All wet preparation of Ag-As33S67 thin films by silver ions photodiffusion from silver nitrate solution. *Journal of Non-Crystalline Solids*. Volume 622, 2023, 122652. DOI: 10.1016/j.jnoncrysol.2023.122652

All wet preparation of Ag-$As_{33}S_{67}$ thin films by silver ions photodiffusion from silver nitrate solution

Michal Kurka,[1,*] Karel Palka,[1,2] Jiri Jancalek,[1] Stanislav Slang,[1] Jakub Houdek,[1]and Miroslav Vlcek[1,2]
[1] Center of Materials and Nanotechnologies, Faculty of Chemical Technology, University of Pardubice, Studentska 95, Pardubice 532 10, Czech Republic
[2] Department of General and Inorganic Chemistry, Faculty of Chemical Technology, University of Pardubice, Studentska 95, Pardubice 532 10, Czech Republic
*michal.kurka@upce.cz

Abstract

Amorphous $As_{33}S_{67}$ thin films were prepared by spin-coating method from n-butylamine based glass solution as well as by thermal evaporation. Thin films were doped by silver ions from a solution of silver nitrate in dimethylsulfoxide. The influence of illumination on the photodoping kinetics was studied in dependence on the deposition technique and thermal pre-history of solution processed $As_{33}S_{67}$ thin films. Doped thin films maintained good optical quality, decreased optical bandgap and increased refractive index were observed with increasing silver content. Highly doped thin films remained amorphous. A hypothesis explaining observed significant differences in doping mechanisms between solution processed and thermally evaporated samples was proposed based on structural differences and organic residua content. Described procedure simplifies the silver doping technique and our findings proved, that it is suitable for all wet processes, thus excluding the necessity for vacuum deposition of solid silver film.

1. Introduction

Chalcogenide glasses are well known materials with high refractive index and wide transparency in the infrared region. These materials, often in a thin film (TF) form, are widely used for manufacturing of optical elements (e. g. diffractive gratings, planar optical waveguides or microlens arrays) [1,2]. Various deposition methods are suitable for the preparation of vitreous chalcogenide TFs. These techniques can be divided into two main groups. The first group consists of physical deposition techniques (e.g. vacuum thermal deposition [3], sputtering [4], laser or electron beam ablation [5], etc.). The second group contains solution-based techniques (e.g. spin-coating [6], spiral bar-coatings [7], electrospray [8], inkjet printing [9], etc.). Solution based techniques demand good solubility of the source bulk chalcogenide glass in used solvents. In the case of chalcogenide glasses, aliphatic amines are frequently applied [10], alternatively their mixture with methanol [11] or with thiols [12]. One of the main disadvantages of solution processed chalcogenide TF is the residual content of organic solvents, which leads to a decrease in refractive index [13]. However, the amount of residual organic solvent entrapped in the structure can be significantly reduced by proper post-deposition thermal treatment [14,15].

The optical properties of chalcogenide TFs can be significantly modified even after the TF deposition by silver ion enrichment, usually performed by photodoping [16-18]. The refractive index of silver-doped chalcogenide glasses increases as simultaneously optical bandgap decreases. This phenomenon can be used to tailor the optical properties of chalcogenide TFs [19]. The traditional way to dope chalcogenide glasses by silver is optically induced diffusion and dissolution of elemental silver TF preparation on the surface of chalcogenide glass [19]. This method of doping requires the deposition of silver TF on the surface of chalcogenide glass, usually by thermal evaporation or sputtering. Alternative source of silver ions can be a solution that contains silver salt [20-22]. In published works [20-22], water was used as a solvent, which can be problematic choice in the case of doping chalcogenide glasses sensitive to hydrolysis. This problem should be resolved by the usage of an aprotic solvent like dimethylsulfoxide. In the case of solution processed TFs of chalcogenide glass, the silver ions can be introduced directly into the source glass solution without the necessity for consecutive photodiffusion [15]. Nevertheless, this process has

certain limitations in silver content in the source glass solution in order to still remain stable without the precipitation of silver rich particles.

In this paper, we studied the possibility of optical properties tailoring by silver ions photodoping of solution processed $As_{33}S_{67}$ TFs prepared by spin-coating (SC). Vacuum thermally evaporated (VTE) TFs of the same composition and thickness were studied as well, in order to compare the photodoping mechanisms with solution processed TFs. Although, silver photodoping is a well-studied phenomenon, we offer a novel approach which has the potential to surpass previously discussed doping methods. In our study, silver doping was performed by photodoping from the solution of silver nitrate in dimethylsulfoxide. As the non-aqueous and anhydrous solvent, dimethylsulfoxide offers a suitable alternative to avoid undesirable chalcogenide glass hydrolysis [2] and due to the nature of solution based doping process, it circumvents the need for preparation of source solid silver TF. The obtained data show the influence of silver content on the composition, structure, optical properties and surface roughness of VTE and spin-coated TFs. The connection of solution based deposition of chalcogenide TFs and their doping from the silver salt solution leads to all wet procedure for gradual tailoring of optical properties of TFs eliminating the need for traditionally used vacuum deposition equipment.

2. Experimental

Source $As_{33}S_{67}$ bulk glass was prepared by the standard melt quenching method. Required amounts of high purity (5N) elements were weighed into a cleaned silica ampoule which was consecutively evacuated ($\sim 10^{-3}$ Pa) and sealed. Sealed ampule was placed into a rocking tube furnace and then heated at 850°C for 32 hours. Ampoule was quenched in cold water.

The first set of TFs samples was prepared by spin-coating method on soda-lime microscopic slides (substrates). For spin-coating method, bulk chalcogenide glass was crushed in agate bowl and then dissolved in n-butylamine. Concentration of glass was 0.1 g of glass per 1 ml of n-butylamine. After the complete dissolution of bulk glass, no turbidity or precipitates were observed in obtained chalcogenide glass solution. Spin-coater SC110 (BEST TOOLS) was used for the deposition of TFs. Freshly prepared TFs were stabilized on hot plate for 20 minutes at 60°C (hereinafter referred as "as-prepared" TFs). As-prepared TFs were subsequently annealed in argon atmosphere at 100°C and/or 140°C for 1 hour to reduce the content of organic residuals and to polymerize fragmented glass structure. The maximum annealing temperature was chosen with respect to the glass transition temperature of source bulk glass (T_g = 145°C [23]). Rotation speeds were set at 2750 rpm and 3000 rpm and rotation time was 120 s. The specific rotation speeds were based on a preliminary experiment to reach approx. 280 nm thickness of all SC TFs before silver doping (i.e. to take into account the expected thermo-induced contraction during annealing shrinkage). The thickness was evaluated from transmission spectra by the procedure described in [24]. The standard deviation of the thickness of studied thin films was ±10 nm for SC as-prepared TFs, ±18 nm for SC TFs annealed at 100 °C and ± 16 nm for SC TFs annealed at 140 °C.

The second set of TFs samples was thermally evaporated using UP-858 (TESLA) evaporating device. Soda-lime microscopic slides were again used as substrates. The process of thermal evaporation was performed at $\sim 10^{-3}$ Pa and the deposition speed was ~1.3 nm/s. The targeted thickness of TFs was ~280 nm to match the targeted thickness of SC TFs. The thickness 280 nm was chosen with regard to the electron beam penetration depth during EDS analysis and to maintain the optical quality of the SC layers. Evaporation rate and thickness were controlled in situ by the quartz crystal microbalance method using STM-2 device (INFICON). The standard deviation of the thickness of thermally evaporated thin films was ± 9 nm.

Solution for TFs silver doping was prepared by dissolving of 0.1 g of silver nitrate in 1 ml of dimethylsulfoxide. Dimethylsulfoxide was chosen as an anhydrous solvent to protect studied TFs against undesirable hydrolysis. TFs of $As_{33}S_{67}$ composition were submerged in 150 µl of the solution containing silver ions. The doping procedure was performed without stirring. The doping kinetics of silver ions were

measured with and without halogen lamp illumination (the light beam illuminates the substrate´s side of the sample). After doping procedure, TFs were treated with pure dimethylsulfoxide and dried by compressed dry air. The TFs doped under the illumination were subsequently exposed to a halogen lamp for homogenization of silver distribution in depth of chalcogenide TFs. Exposure times were determined based on the evaluation of transmission spectra of treated TFs – i.e. the TFs with homogeneous depth distribution of the silver reached the transmission of the substrate in their interference maxima. Particular exposure times are provided in supplementary material Table S1. Subsequently, silver photodoped TFs were annealed in an argon atmosphere at 140°C for 1 h to remove organic residua.

Kinetics of photodoping (doping with illumination) were measured in situ. Fiber UV-VIS spectrometer EPP2000 (STELLARNET) was used for the measurement of transmittance spectra by placing optical fiber beyond the doping cell, while halogen lamp was simultaneously used as a light source for doping and optical measurements (after significant attenuation of incoming light beyond the sample). Kinetics of doping without illumination were measured ex situ. Transmission spectra were measured after 10 s, 20 s, 30 s, 40 s, 50 s, 60 s, 120 s (as-prepared SC TFs) and 15 s, 30 s, 45 s, 60 s, 120 s, 300 s, 600 s (VTE and SC annealed at 100°C and 140°C TFs) of submersion in the doping solution by UV-VIS-NIR spectrometer UV3600 (SHIMADZU). The change of absorption coefficient $\Delta\alpha$ at 470 nm was evaluated from transmission spectra according to [25]. Change in optical absorption coefficient Δα is defined as:

$$\Delta\alpha = \frac{ln\frac{T_0}{T_t}}{d} \quad (1),$$

where T_0 is transmittance at 470 nm of sample in the initial state. T_t is transmittance at 470 nm in time t and d is the thickness of TF in meters.

The doping solutions before and after doping process were analyzed by X-ray fluorescence (XRF). XRF spectra were recorded with the device ATLAS X (IXRF SYSTEMS) equipped with rhodium anode. Measurements of each sample (10 µl of solution) were performed at 50 kV acceleration voltage and 500 µA current in ambient atmosphere. The signal was accumulated for 100 s. The obtained data are presented in supplementary material Figures S3, S4, and S5. In XRF spectra, the peaks between 18-22 keV are Compton and Rayleigh peaks produced by the scattering of primary X-ray radiation. The results are presented in the form of a dependence of the As Kα line intensity on the silver content in doped thin film (obtained by EDS, see below). This form was chosen due to the clarity of presented data and the absence of precise arsenic calibration standard for arsenic ions in dimethylsulfoxide.

The composition of source bulk glass and prepared TFs was studied by energy dispersive X-ray spectroscopy (EDS) using AZtec X-Max 20 detector (OXFORD INSTRUMENTS) installed in field emission scanning electron microscope (FESEM) LYRA 3 (TESCAN) equipped by high brightness Schottky emitter. Measurements of each sample were performed on 400x400 µm spots at 5 kV acceleration voltage (or 20 kV for the chalcogenide bulk glass sample). Error bars represent the standard deviation from 15 measurements on three separate samples which underwent the same treatment. Compositions are provided in supplementary material Table S2.

SEM images of all studied thin films were acquired at 10 kV acceleration voltage on the same device (LYRA 3, TESCAN) they are provided in supplementary materials in Figures S6 and S7 of this paper.

Amorphous state of TFs was investigated by XRD measurement. The XRD patterns were measured for the highest doped TFs in EMPYREAN (MALVERN PANALYTICAL) diffractometer equipped by copper anode. The range of measurement was 5 to 90° with step 0.0065651°.

The transmission spectra for evaluating of optical parameters and thickness were measured by UV-VIS-NIR spectrometer UV3600 (SHIMADZU) in the spectral range 190-2000 nm. The thickness and refractive index of TFs were evaluated by the procedure described in [24] based on Wemple-DiDomenico's parametrization of the spectral dependence of refractive index [26] and the model of TF transmission spectra presented by R. Swanepoel [27]. Values of optical bandgap were determined using Tauc´s method for semiconductors [28]. Discussed data of refractive index and optical bandgap represent average values

obtained by measurement and evaluation of three samples of each treatment. Error bars represent the standard deviation of obtained values.

Structure of undoped and doped TFs was investigated by MultiRAM (BRUKER) FT-Raman spectrometer. Raman scattering was excited by 1064 nm Nd:YAG laser. Measurements were performed using beam intensity in the range between 30–40 mW with 2 cm^{-1} resolution and 64 scans averaging. Raman spectra were normalized by the most intensive band in the measured spectrum. The structure of undoped and doped TFs annealed at 140°C could not be studied because of the highly intensive luminescence of annealed samples [29-31]. The structure of doped VTE samples in the range 30.4 – 53.4 at. % of silver and SC TFs annealed at 100°C with the content of silver 46.7 at. % also, could not be studied due to the significant heating of samples.

The surface roughness of prepared TFs was studied by atomic force microscopy (AFM). Measurements were performed with the device NTEGRA (NT-MDT) equipped by pyramidal silicon tip NSG 10 (APPNANO). AFM scans were measured from 5x5 μm area and presented surface roughness values are averaged from 3 measurements. Presented error bars are the standard deviation of calculated mean values.

3. Results and discussion

Samples submerged in doping solution without illumination were investigated first. Dependences of Δα on the submersion time of studied TFs are presented in Fig. 1. All studied samples show similar behavior of Δα changes. We can observe the rapid increase of Δα shortly after the submersion of TFs into the doping solutions. The rapid increase of Δα is followed by stabilization of its values. In [17] increase of Δα (decrease of E_g^{opt}) is connected with the amount of silver in TFs. For this reason, this behavior can be explained by formation of silver rich surface layer on chalcogenide TF which halts further doping. The silver rich layer formation is probably caused by the reaction of silver ions with free sulfur on the surface of thin films. After exhaustion of free sulfur in the surface layer of doped TF the silver ions have no sulfur to further react and the doping process halts. This hypothesis can be supported by the saturation of Δα values which is illustrated in Fig. 1. The formed silver rich layer cannot be diffused to the volume of samples without external energy (e. g. illumination, annealing). In the case of vacuum thermally evaporated (VTE) and spin-coated (SC) samples annealed at 100 and 140 °C we can observe very close values of Δα after formation of silver rich layer. As-prepared SC TFs exhibit a significantly larger change of Δα. Generally, the observed formation of silver rich layer, which involves the reaction of silver ions and free sulfur is in good agreement with previously published works [32,33]. In these works, the reaction of free sulfur and silver ions (supplied from metallic silver thin film) is also the first and necessary step during illumination induced dissolution and diffusion of silver into the chalcogenide thin film.

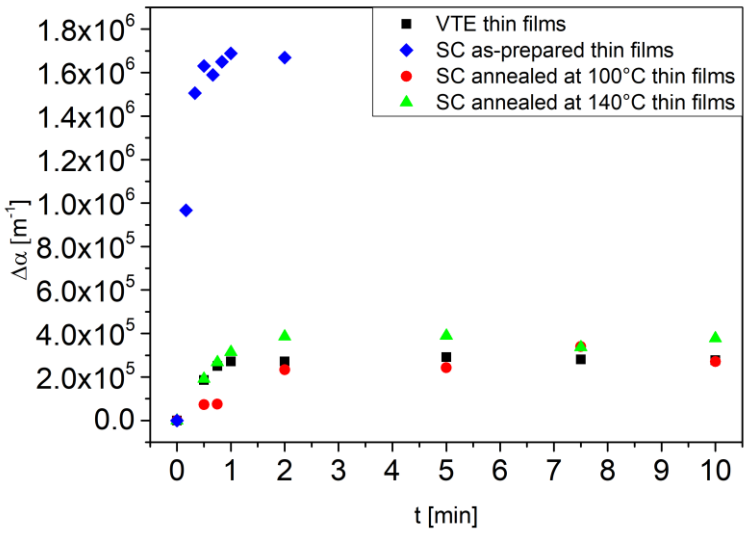

Fig 1.: Dependence of change in optical absorption coefficient Δα of VTE and SC TFs on submersion time during doping by silver ions (without illumination).

For explanation of observed silver doping kinetics (without illumination) of solution processed (SC) $As_{33}S_{67}$ TFs, we propose the following hypothesis. As-prepared SC TFs contain entrapped organic residua of solvent and alkyl ammonium arsenic sulfide salts originating from the glass dissolution process. During thermal stabilization treatment, organic salts are decomposed and together with entrapped solvent they are released from TF matrix. The amount of removed organic residua quickly increases with increasing annealing temperature, but they cannot be completely removed. Simultaneously, the structure of SC TF is getting more polymerized [34,35]. The surface layer of the annealed SC TF is significantly depleted in organic residua content and highly polymerized [35] so we can assume that its properties are close to those of VTE TFs. Thus, a similar silver rich surface layer is formed on the surface of annealed SC TFs as in the case of VTE film. Contrary, as-prepared SC TFs lack the highly polymerized surface layer because the stabilization was performed at a lower temperature (60°C) which is below the boiling point of the n-butylamine. Progress of the silver diffusion is not limited by the surface highly polymerized layer of the glass. Moreover, the structure of as-prepared SC TF is formed by weakly polymerized nanoclusters of glass (terminated with alkyl ammonium arsenic sulfide salts), sulfur rich areas (sulfur chains and rings in between sulfur terminated glass clusters) and the content of residua organic solvents is significantly higher in comparison with annealed SC TFs. For these reasons silver ions can migrate deeper into the TF (in higher concentration), which results in the larger increase of $\Delta\alpha$ coefficient.

The absorption coefficient changes of TFs doped by silver ions under illumination (hereinafter referred as photodoped) are presented in dependence on the time of submersion in the doping solution in Fig. 2. Data from TF doping by silver ions without illumination (given in Fig. 1) are presented in Fig. 2 as well for comparison with the photodoping process. Fig. 2 gives evidence that illumination significantly magnifies changes of absorption coefficient (larger differences of Δα with illumination in comparison without illumination). This behavior can be interpreted as increase of doping rate by silver ions. It is in a good agreement with [32] where increase of illumination intensity caused increase of doping rate by silver in VTE TFs. We can observe that the kinetics of photodoping by silver ions from solution are different for VTE and SC TFs. In the case of VTE TFs the kinetics of doping is similar as doping from solid TFs of silver [32]. Time dependence of doping of VTE TFs can be divided into two parts. The first one is the exponential part where silver ions react with free sulfur giving silver sulfide. In the second part (linear), the photodoping is

slower. It is caused by small differences between the chemical potentials of the doped and undoped part of the TF [32,33].

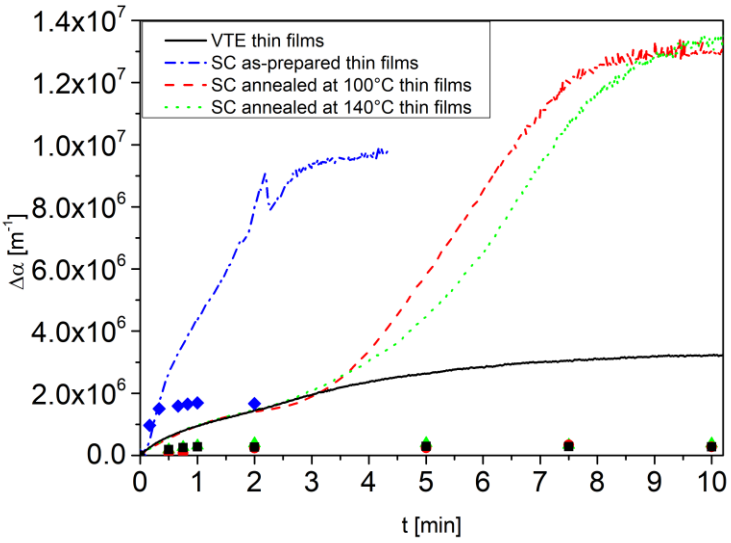

Fig. 2: Dependence of change in optical absorption coefficient Δα of VTE and SC TFs on submersion time during photodoping by silver ions (measured in situ). Scatter points represent silver doping without illumination (measured ex situ).

The kinetic of SC TFs photodoping is significantly more complex. We can observe the same exponential part at the beginning of the photodoping process as in the case of VTE TFs. Contrary to the VTE TFs the value of absorption coefficient change doesn't remain stable but after the short linear part follows the second exponential part of steep change of absorption coefficient increase ending with saturation. The onset of the second exponential growth of photodoping kinetic is shifted to later times with increasing annealing temperature of SC TFs.

These observations are consistent with our theory proposed above. The first exponential part of the curve corresponds to the reaction of silver ions with free sulfur [32,33] inside the highly polymerized layer atop of the SC TFs, which is structurally similar to VTE films. For this reason, we observe similar doping kinetics at the beginning of the doping process as in the case of VTE TFs. This first exponential part is practically missing in the case of as-prepared SC TFs which didn't undergo any consequent annealing at higher temperatures and thus no highly polymerized surface layer is present.

Once the silver ions diffuse through polymerized surface layer (diffusion is accelerated by illumination) it starts to diffuse through the part of the TF which contains organic residua. Presence of organic residua and specific structure of SC TFs formed by polymer matrix and sulfur rich areas (sulfur chains and rings in between sulfur terminated glass clusters) [34,36,37] significantly accelerate the silver ion diffusion process. Once the TF becomes fully doped with silver ions the change of absorption coefficient kinetics reaches saturation.

It was observed that samples highly doped with silver possessed worsened adhesion to the substrates. Because of this reason the only samples which were fully attached to the substrates after the drying process, as described in the experimental section were taken for further experiments. Maximal content of silver in studied TFs was 37.04 at. % (as-prepared SC TFs), 46.7 at. % (SC TFs annealed at 100 °C), 20.8 at. % (SC TFs annealed at 140 °C) and 53.4 at. % (TVE TFs).

Content of silver in photodoped $As_{33}S_{67}$ TFs was studied by EDS. Composition of source bulk glass was measured by EDS too and the results of the measurement are provided in supplementary materials Table S2. Dependence of silver content on the time of photodoping is given in Fig. 3. It was verified that the increasing of Δα is directly connected with silver content in the TFs (Fig. 2). In the case of VTE TFs, after ~4.5 minute of exposure the amount of silver is approximately 45 at. % and exponential part of photodoping kinetic is changed to linear part. This result is in good agreement with observation from in situ measurement of photodoping kinetic (Δα) in VTE TFs (Fig. 2). In the case of SC TFs we can observe shift of steep silver content increase to the longer times with increasing temperature of annealing. It is also in good agreement with data observed from optical measurement of photodoping kinetics (Fig. 2) and with proposed hypothesis.

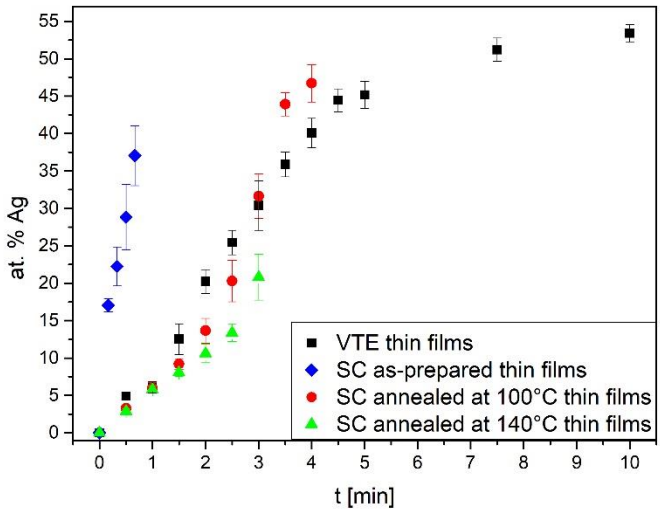

Fig. 3: Dependence of silver content in VTE and SC TFs on the time of photodoping.

The used doping solutions isolated after doping processes were studied by XRF. The similar concentration of silver ions was confirmed in doping solutions analyzed before and after the doping process with illumination (similar values of intensity Ag Kα line in XRF spectra Fig. S4). It gave evidence that the concentration of silver ions in doping solution was large enough, that the illumination-induced doping process would not be affected by a negligible decrease of silver content in used solution.

The XRF spectra of solutions obtained after doping procedure confirm the presence of typical As Kα line (Fig. S4). At first, the studied VTE TF was submerged in pure dimethylsulfoxide and kept for 10 min under illumination to determine the influence of pure solvent. Fig. S5 confirms that submersion in pure dimethylsulfoxide induces only minor leaching As-based structural units.

Subsequently, all used silver doping solutions (after photo-doping) were analyzed as well. The As content in doping solutions is presented in Fig. 4 as a dependence of As Kα line intensity on Ag content in studied TFs (determined by EDS, see above). The data are also compared with As content in doped thin films. Fig. 4 shows that with increasing content of silver in studied TFs, the concentration of arsenic in used solutions is gradually increasing. It signifies that silver photo-doping is also accompanied by partial leaching of As structural units into the solution of silver nitrate in dimethylsulfoxide. Simultaneously the EDS data confirm decrease of As-content in studied thin films as well.

We assume that arsenic depletion in TFs is related to changes in structure and this phenomenon is connected with the formation of As_4S_4 clusters with increasing content of silver in ChG TF matrix. The formation of As_4S_4 clusters in silver-doped glass was also previously observed by [38,39]. We assume that

As_4S_4 cage-like clusters which are not directly bonded with polymer matrix of TFs can be washed out into the dimethylsulfoxide solution during silver ions photodoping. Our theory based on the leaching of As_4S_4 can explain the weak As Kα line in used pure dimethylsulfoxide (Fig. S5), because the structure of As-S VTE TFs contains a significant amount of As_4S_4 clusters [10].

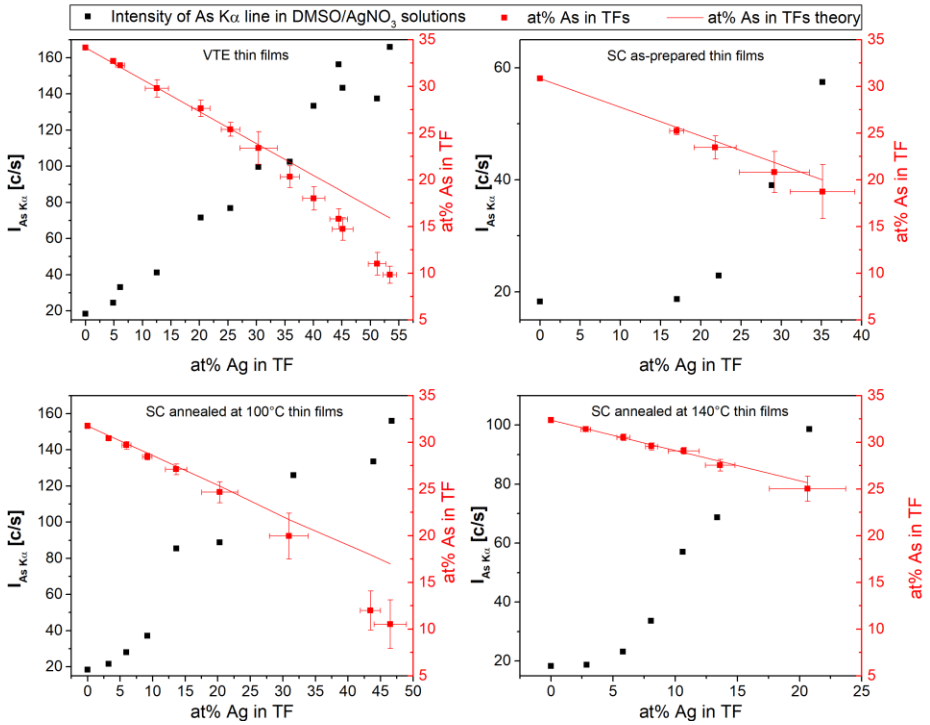

Fig. 4: Dependences of As content in TFs and intensities of As Kα line in doping solution after doping process on content of Ag in TFs.

The composition of the glassy matrix in form of As/S ratio is provided in Fig. 5. The data are presented as dependence of As/S ratio on the silver content. It was noted that TFs deposited by SC method (before silver doping) are slightly depleted in arsenic in comparison with their VTE counterparts, which is in good agreement with previously published results [40]. From Fig. 5, we can observe arsenic depletion which relates to increasing the content of silver and starts at ~25 at. % of silver. Arsenic depletion is dependent on the amount of silver in TFs, not on time of doping nor on used TF deposition technique. In Fig. 5, we can observe that arsenic depletion is observable in TFs at similar concentration of silver. As we mentioned above, we assume that arsenic depletion relates to the leaching of As_4S_4 clusters with increasing content of silver in ChG TF matrix. Formation of As_4S_4 clusters in silver-doped glass was also previously observed by [38,39].

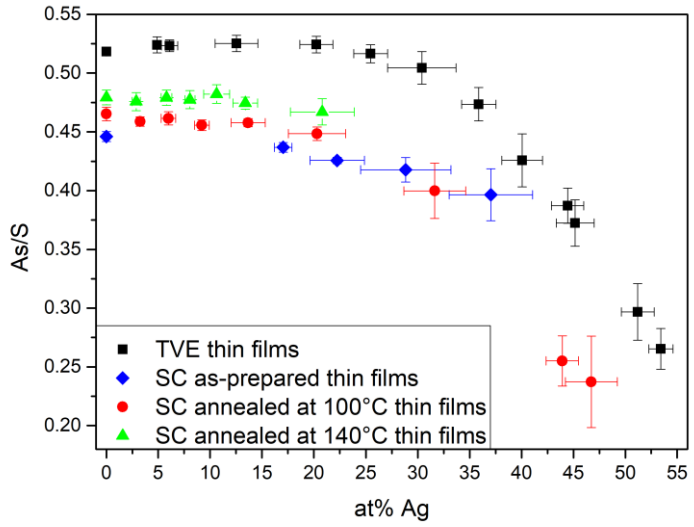

Fig. 5: Dependence of As/S ratio on silver content in photodoped TFs.

Amorphous state of TFs with the highest silver content (i.e. 37.04 at. % in as-prepared SC TFs, 46.7 at. % in SC TFs annealed at 100 °C, 20.8 at. % in SC TFs annealed at 140 °C and 53.43 at. % in TVE TFs) was investigated by XRD analysis. The obtained XRD patterns are shown in Fig. 6. From the presented XRD patterns we assume that even the highest photodoped TFs are still amorphous, respectively high concentration of silver in the TFs does not cause crystallization. We can observe only two weak peaks at 13.852° and 27.912° in XRD spectra of VTE TFs and in SC TFs annealed at 140 °C. These peaks correspond to the cubic modification of crystalline arsenic oxide As_4O_6 (ICDD:01-084-7609). The presence of As_4O_6 can be explained by partial oxidation of the TF surface. The minor oxygen content can be explained eighter by storage before EDS analysis (for VTE TF) or by partial oxidation probably initiated by a small amount of residual oxygen in the annealing chamber (for SC TF annealed at 140°C) as As-S thin films are naturally prone to surface hydrolysis and oxidation [2].

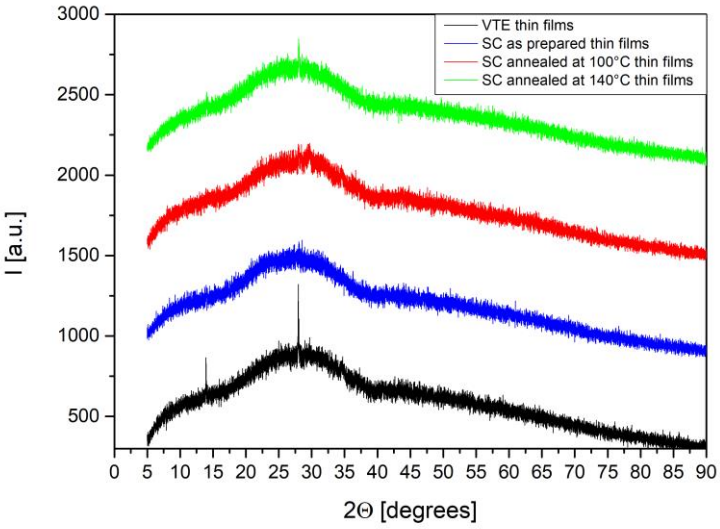

Fig. 6: XRD patterns of TFs with the highest amount of silver.

Optical quality of prepared TFs was assessed from UV-VIS-NIR transmission spectra. Fig. 7 presents transmission spectra of undoped TFs, TFs with the highest content of silver without loss of optical quality and the first TFs in the concentration row without specular optical quality. However, almost all TFs doped by silver were prepared in good optical quality. In the case of VTE TFs (Fig. 7 A) and SC TFs doped after annealing at 140°C (Fig. 7 D), good optical quality was acquired in full studied concentration range of silver doping (VTE TFs in range 0 – 53.4 at. % of silver and SC TFs annealed at 140 °C in range 0 – 20.8 at. % of silver). SC silver doped as-prepared TFs (Fig. 7 B) possessed good optical quality in the range 0 – 22.2at. % of silver and SC TFs silver doped after annealing at 100°C (Fig. 7 C) were obtained in good optical quality in the range 0 – 31.6 at. % of silver.

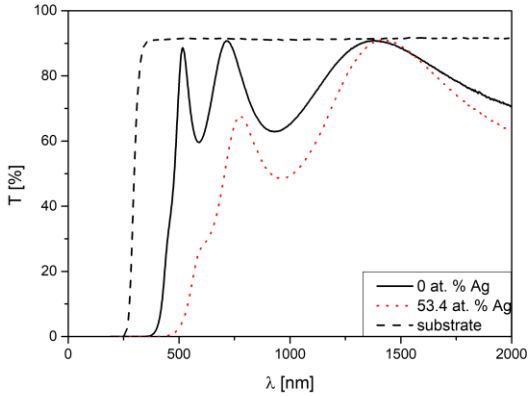

A: VTE TFs

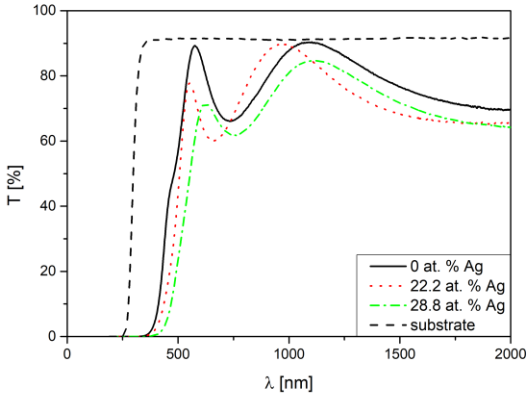

B: As-prepared SC TFs

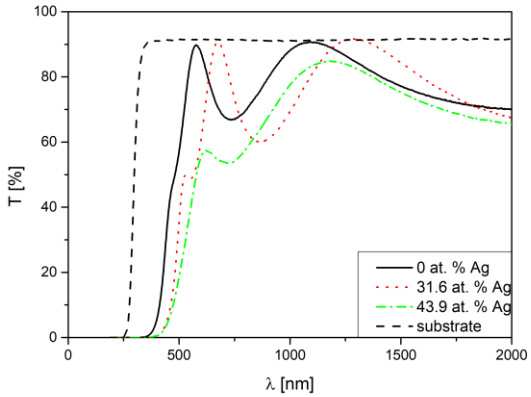

C: Annealed at 100°C SC TFs

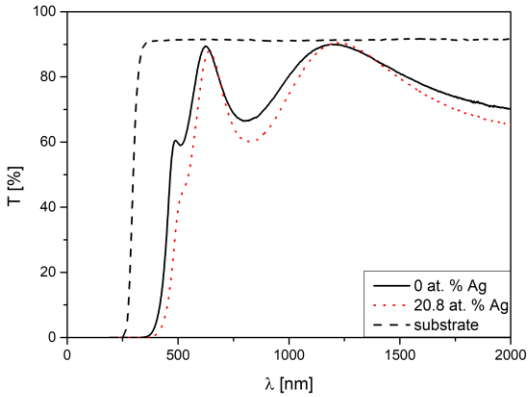

D: Annealed at 140°C SC TFs

Fig. 7: Transmittance spectra of VTE and SC TFs after various thermal and silver photodoping treatments (for details refer to main text).

Loss of specular optical quality of TFs can be mainly associated with significant changes of their surface roughness as we can observe the increase of surface roughness with increasing silver content after photodoping (Fig. 7). In the case of VTE TFs and SC TFs annealed at 140°C there is only a slight increase of surface roughness with the increase of silver content and this increase did not significantly influence films optical quality. As-prepared SC TFs show steep increase of surface roughness with increasing content of silver. This significant increase can be connected with low chemical resistance of as-prepared SC TFs and with changes in the structure of TFs (will be discussed later). Noteworthy increase of surface roughness

was observed in the case of SC TFs annealed at 100°C too, this increase starts between 20 and 30 at. % of silver. We assume that increase of surface roughness is connected with steeper increase of silver content in the second exponential part of photodoping (Fig. 3). Our theory is based on the leaching of As_4S_4 clusters from TFs which relates to increasing of silver content. The leaching of As_4S_4 structural units is confirmed by XRF analyses as well. As discussed before, the data shows increasing intensity of As Kα line with increasing silver content in TFs (Fig. 4). SEM images of all studied TFs are shown in supplementary materials Figures S6 and S7.

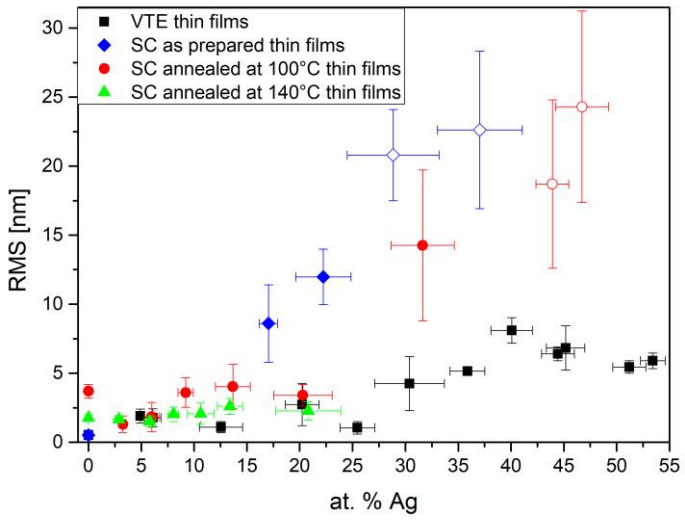

Fig. 7: Dependence of surface roughness on content of silver. Hollow points indicate TFs without specular optical quality.

Measured transmission spectra were evaluated by the procedure described in the experimental part of the paper and obtained dependences of optical bandgap and refractive index (at 1550 nm) on silver concentration are given in Fig. 8. With increasing amounts of silver optical bandgap decreases in all studied samples. Decrease of optical bandgap can be explained by replacing of As-S and S-S bonds for Ag-S bonds which have lower binding energy [19]. We can observe that the refractive index increases with increasing content of silver in TFs. VTE TFs show higher refractive index than SC TFs. This fact is caused by the presence of organic residua trapped in SC TFs and by differences in the structure of VTE and SC TFs [41]. SC TFs (as well as VTE ones) of all treatments were annealed at 140°C before measurement of transmission spectra. For this reason, the values of the refractive index are similar for undoped SC TFs. In the case of SC TFs, we observe increase of refractive index with the temperature of annealing before photodoping of SC TFs, the same behavior of refractive index on the temperature of annealing is observed in undoped SC TFs in [41]. In [41] dependences of refractive index on the temperature of annealing are explained by decreasing organic residua content with increasing temperate of annealing. From our observation, we assume that during silver photodoping, a certain amount of organic residua is preserved in SC TFs and it is not possible to remove these organic residua by annealing after photodoping – refractive index of SC samples pre-annealed at 140°C is still higher than the refractive index of samples pre-annealed at 100°C even after post-doping annealing of all samples at 140°C.

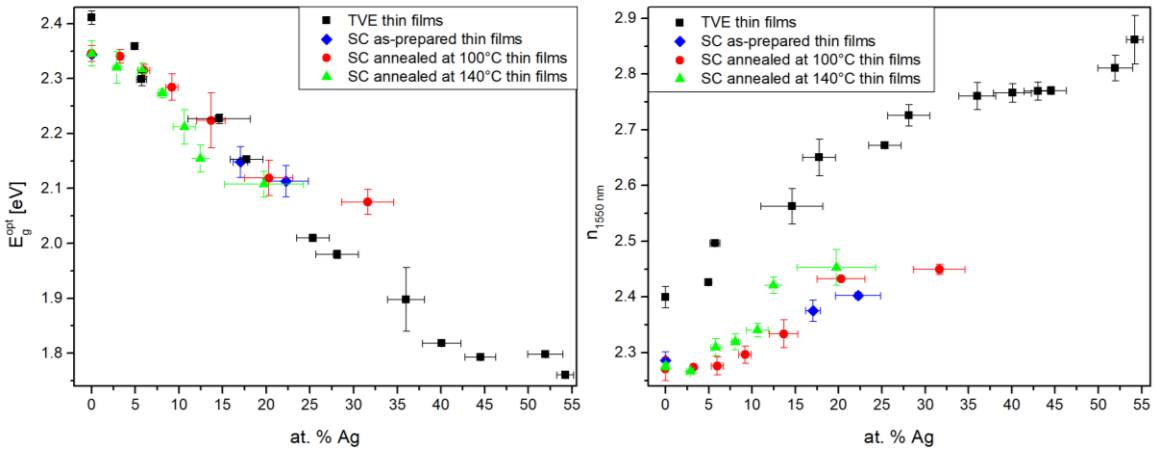

Fig. 8: Dependence of optical bandgap (left) and refractive index at 1550 nm (right) on silver concentration.

Structure of undoped and doped TFs was studied by Raman spectroscopy (Fig. 9). The main band in Raman spectra of undoped TFs at 344 cm^{-1} correspond to vibration of trigonal pyramidal structure $AsS_{3/2}$ [42-44], which is also the main structural unit in the doped TFs matrix. Another significant bands in Raman spectra of undoped TFs corresponds to S_8 rings (475 cm^{-1}) [43,45,46] and S-S chains (495 cm^{-1}) [47,48,49]. We can observe both bands in Raman spectra of VTE and SC TFs. Band associated with structure S-S chains is more pronounced for VTE TFs. Contrary, band corresponding with S_8 rings is more pronounced for SC TFs. In the case of as-prepared SC TFs before doping by silver, we observe band at 415 cm^{-1}, which belong to the vibrations of alkyl ammonium arsenic sulfide (AAAS) salts [40,47,48], which were created during the dissolution of bulk glass in n-butylamine. AAAS salts are thermally labile and after annealing TFs at 100°C their decomposition occurs. This can be observed in Raman spectra of SC TFs annealed at 100°C where band at 415 cm^{-1} appears at significantly lower intensity in comparison with the Raman spectrum of as-prepared SC TFs [47]. In the Raman spectra of as-prepared SC TFs, we can observe band at 375 cm^{-1}, this band can be assigned to As_4S_4 clusters [42,44,50]. After annealing of SC TFs, intensity of band at 375 cm^{-1} and 475 cm^{-1} decreases, as a result of thermoinduced polymerization process in as-prepared SC TFs after annealing.

After silver ions photodoping, we observe increase of band at 375 cm^{-1}, which can be assigned to S-Ag-S linkage in the structure of $AsS_{3/2}$ pyramids connected by silver and to AgS_3 pyramidal structural units [15,17,38]. As described above, band 375 cm^{-1} can be also assigned to As_4S_4 clusters. Due to the overlapping bands of S-Ag-S linkage and As_4S_4 clusters, we can not distinguish these two structural units, but formation of clusters As_4S_4 was observed in [38,39], as already mentioned. We believe that combination of these two structural changes, the formation of Ag-S bonds and As_4S_4 clusters, causes significant intensity increase of band at 375 cm^{-1}.

In the case of as-prepared SC TFs, we observed disappearance of band at 415 cm^{-1} after photodoping by silver (even at lowest silver concentration). This phenomenon can be explained by the decomposition of AAAS salts by reaction with silver ions, which initiated creation of Ag-S bonds. We assume that Ag-S bonds are more stable than bonds in AAAS salt. This behavior is in good agreement with our hypothesis that organic compounds in the matrix of TF accelerate photodoping by silver.

Due to doping by silver, we can observe the increase in the intensity of band at 375 cm^{-1} and decreasing intensity of bands assigned to S_8 and S-S chain structures (both for VTE and SC TFs). This phenomenon can be explained by creating new bond between silver and sulfur. From Raman spectra of studied TFs we can assume that during photodoping sulfur chains are preferred for reaction with silver ions. This conclusion

is based on the preferential decrease of the intensity of band at 495 cm^{-1} (S-S chains) in comparison with the band at 475 cm^{-1} (S_8 rings). We can observe this behavior in the case of all studied samples and treatments.

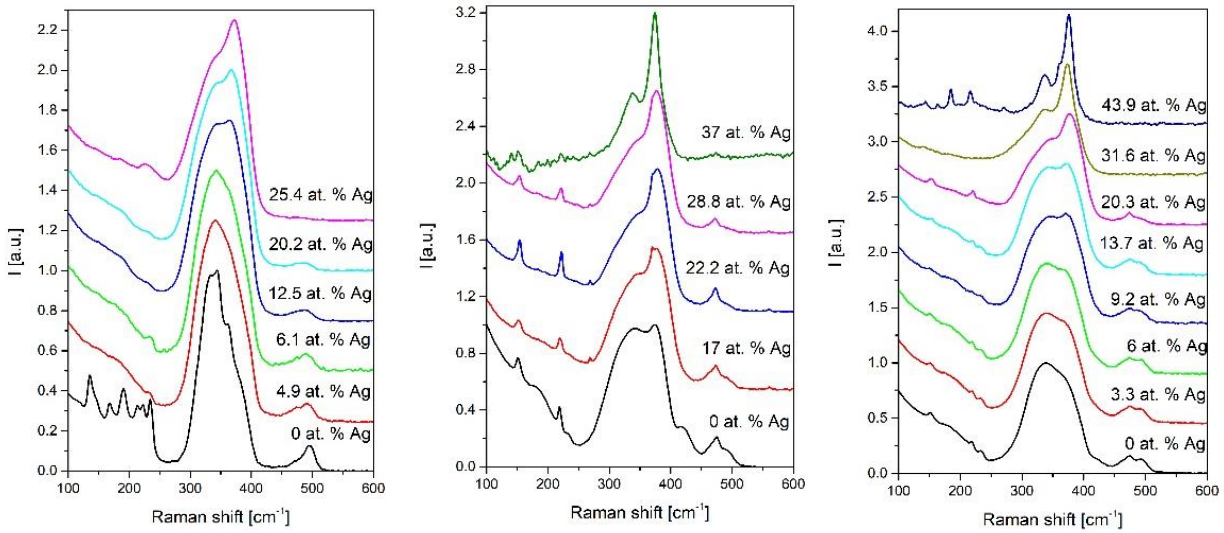

TVE SC TFs as-prepared SC TFs annealed at 100°C

Fig. 9: Raman spectra of TVE and SC TFs before and after doping by silver.

4. Conclusion

The $As_{33}S_{67}$ thin films (TFs) prepared by spin-coating (SC) and vacuum thermal evaporation (VTE) were doped by silver ions from the solution of silver nitrate in dimethylsulfoxide both under and without halogen lamp illumination. We observed significantly different kinetics of photodoping for VTE and SC TFs. The Raman spectroscopy showed significant changes in films structure induced by silver ions photodoping. Based on observed data, we believe that organic compounds in SC TFs and the specific structure of SC TFs formed by polymer matrix and sulfur rich areas accelerate the photodoping process. Detailed hypothesis explaining observed phenomena was proposed.

The differences between SC and VTE thin films can be explained by their significant difference in structure. As-prepared SC TFs contain entrapped organic residua of residual solvent molecules and alkyl ammonium arsenic sulfide salts originating from the glass dissolution process. During thermal stabilization treatment, organic salts are decomposed and together with entrapped solvent, they are released from TF matrix. The amount of removed organic residua quickly increases with increasing annealing temperature, but they cannot be completely removed. Moreover, the structure of SC TFs is formed by polymer matrix and sulfur rich areas (sulfur chains and rings in between sulfur terminated glass clusters). On the contrary, the VTE thin films possess highly disordered structure and no organic residuals. For this reason, the presence of organic residuals and specific structure can still influence photodoping process of silver ion into SC annealed TFs.

Majority of doped thin films maintained good optical quality. Decrease of optical bandgap and increase of refractive index with increasing amount of silver in all studied TFs was observed. Even highly doped thin films remained amorphous. With increasing content of silver above ~25 at. % in TFs decreasing content of arsenic was observed probably due to leaching of the As_4S_4 clusters out to the doping solution, which was also confirmed by XRF analysis of used doping solutions.

Obtained results proves that optical parameters of chalcogenide TFs can be gradually altered by silver ion photodoping by all wet process without the need for vacuum deposition techniques for source silver

film deposition. It is possible to enrich the chalcogenide TFs by the high content of silver (~45 at. % silver) in one step, which is not achievable from single vacuum deposited solid silver film.

Acknowledgement

Authors appreciate financial support from grant LM2023037 from the Ministry of Education, Youth and Sports of the Czech Republic and European Regional Development Fund-Project "High-sensitive and low-density materials based on polymeric nanocomposites – NANOMAT" (CZ.02.1.01/0.0/0.0/17_048/0007376).

References

[1] Tanaka K., Shimakawa K., *Amorphous Chalcogenide Semiconductors and Related Materials*, Springer-Verlag: New York, NY, 2011.

[2] Adam J.L., Zhang X., *Chalcogenide glasses: Preparation, properties and applications*, Woodhead Publishing: Oxford, GB, 2014.

[3] Gonzáles-Leal J.M.; Stuchlik M.; Vlcek M.; Jiménez-Garay R.; Márquez E., Influence of the deposition technique on the structural and optical properties of amorphous As S films. *Appl. Surf. Sci.* **2005**, 246, 348-355.

[4] Balan V.; Vigreux C.; Pradel A., Chalcogenide thin films deposited by radio-frequency sputtering. *J. Optoelectron. Adv. Mater.* **2004**, 6, 875-882.

[5] Youden K. E.; Grevatt T.; Eason R. W.; Rutt H. N.; Deol R. S.; Wylangowski G., Pulsed laser deposition of Ga-La-S chalcogenide glass thin film optical waveguides. *Appl. Phys. Lett.* **1993**, 63, 1601.

[6] Chern G.C.; Lauks I., Spin coated amorphous chalcogenide films: Thermal properties. *J. Appl. Phys.* **1983**, 54, 4596.

[7] Palka K.; Syrovy T.; Schröter S.; Bruckner S.; Rothhardt M.; Vlcek M., Preparation of arsenic sulfide thin films for integrated optical elements by spiral bar coating. *Opt. Mater. Express* **2014**, 4, 384-395.

[8] Novak S.; Lin P.T.; Li Ch.; Lumdee Ch.; Hu J.; Agarwal A.; Kik P.G.; Deng W.; Richardson K., Direct Electrospray Printing of Gradient Refractive Index Chalcogenide Glass Films. *ACS Appl. Mater. Interfaces* **2017**, 9, 26990-26995.

[9] Sanchez E.A.; Waldmann M.; Arnold C.B., Chalcogenide glass microlenses by inkjet printing *Appl. Opt.* **2011**, 50, 1974-1978.

[10] Jancalek J.; Palka K.; Kurka M.; Slang S.; Vlcek M., Comparison of solution processed As33S67 thin films deposited using primary amines of various aliphatic chain length. *J. Non-Cryst. Solids* **2020**, 550, 120382.

[11] Slang S.; Palka K.; Jancalek J.; Kurka M.; Vlcek M., Deposition and characterization of solution processed Se-rich Ge-Se thin films with specular optical quality using multi-component solvent approach. *Opt. Mater. Express* **2020**, 10, 2973-2986.

[12] McCarthy C.L.; Brutchey R.L. Solution processing of chalcogenide materials using thiol–amine "alkahest" solvent systems, *Chem. Commun.* **2017**, 53, 4888-4902.

[13] Palka K.; Jancalek J.; Slang S.; Grinco M.; Vlcek M., Comparison of optical and chemical properties of thermally evaporated and spin-coated chalcogenide As–S thin films targeting electron beam lithography applications. *J. Non-Cryst. Solids* **2019**, 508, 7-14.

[14] Song S.; Dua J.; Arnold C. B., Influence of annealing conditions on the optical and structural properties of spin-coated As_2S_3 chalcogenide glass thin films. *Opt. Express* **2010**, 18, 5472-5480.

[15] Wagner T.; Kohoutek T.; Vlcek Mir.; Vlcek Mil.; Munzar M.; Frumar M., Spin-coated $Ag_x(As_{0.33}S_{0.67})_{100-x}$ films: Preparation and structure. *J. Non-Cryst. Solids* **2003**, 326&327, 165-169.

[16] Kosa T. I.; Wagner T.; Ewen P.J.S.; Owen A.E., Index of refraction of Ag-doped $As_{33}S_{67}$ films: measurement and analysis of dispersion. *Philos. Mag. Part B* **1995**, 71, 311-318.

[17] Krbal M.; Wagner T.; Kohoutek T.; Vlcek Mir.; Vlcek Mil.; Frumar M., Optical properties and structure of amorphous $Ag_x(As_{0.33}S_{0.67})_{100-x}$ Films prepared by optically- induced diffusion and dissolution of silver into spin-coated amorphous $As_{33}S_{67}$ films. *J. Optoelectron. Adv. Mater.* **2003**, 5, 1147-1153.

[18] Viswanathan A.; Thomas S., Tunable linear and non linear optical properties of GeSeSb chalcogenide glass with solute concentration and with silver doping *J. Alloys Compd* **2019,** 798, 424-430.

[19] Krbal M.; Wagner T.; Kohoutek T.; Nemec P.; Orava J.; Frumar M., The comparison of Ag–$As_{33}S_{67}$ films prepared by thermal evaporation (TE), spin-coating (SC) and a pulsed laser deposition (PLD). *J. Journal of Physics and Chemistry of Solids* **2007**, 68, 953-957.

[20] Utsugi Y.; Watanabe Y.; Nagamura T., Spectroscopy of atom movements in photo-excited silver-chalcogenide glasses. *J. Non-Cryst. Solids* **2003**, 326&327, 226-232.

[21] Sakr G.B.; Yahia I.S.; El-Komy G.M.; Salem A.M., Optical properties of thermally evaporated Bi_2Se_3 thin films treated with $AgNO_3$ solution. *Surf. Coat. Technol.* **2011**, 205 3553-3558.

[22] Diliegros-Godines C.J.; Santos Cruz J.; Mathews N.R.; Pal M., Effect of Ag doping on structural, optical and electrical properties of antimony sulfide thin films. *J. Mater. Sci.* **2018**, 53, 11562-11573.

[23] Borisova Z., *Glassy Semiconductors*, Springer-Verlag: New York, NY, 1981.

[24] Palka K.; Slang S.; Buzek J.; Vlcek M., Selective etching of spin-coated and thermally evaporated $As_{30}S_{45}Se_{25}$ thin films. *J. Non-Cryst. Solids* **2016,** 447, 104–109.

[25] Shimakawa K.; Nakagawa N.; Itoh T., The origin of stretched exponential function in dynamic response of photodarkening in amorphous chalcogenides. *Appl. Phys. Lett.* **2009**, 95, 051908.

[26] Wemple S.H.; DiDomenico M., Behavior of the Electronic Dielectric Constant in Covalent and Ionic Materials. *Phys. Rev. B* **1971,** 3, 1338–1351.

[27] Swanepoel R., Determination of the thickness and optical constants of amorphous silicon. *J. Phys. E Sci. Instrum.* **1983,** 16, 1214.

[28] Tauc J., Absorption edge and internal electric fields in amorphous semiconductors. *Mat. Res. Bull.* **1970,** 5, 721–729.

[29] S. Slang, P. Janicek, K. Palka, M. Vlcek, Structure and properties of spin-coated $Ge_{25}S_{75}$ chalcogenide thin films, Opt. Mater. Express **2016**, 6 1973-1985.

[30] S. Slang, K. Palka, H. Jain, M. Vlcek, Influence of annealing on the optical properties, structure, photosensitivity and chemical stability of As30S70 spin-coated thin films. J. Non-Cryst. Solids **2017,** 457 135-140.

[31] S. Slang, P. Janicek, K. Palka, L. Loghina, M. Vlcek, Optical properties and surface structuring of $Ge_{20}Sb_5S_{75}$ amorphous chalcogenide thin films deposited by spin-coating and vacuum thermal evaporation. Mater. Chem. Phys. **2018,** 230 310-318.

[32] Wagner T.; Krbal M.; Kohoutek T.; Perina V.; Vlcek Mir.; Vlcek Mil.; Frumar M., Kinetics of optically- and thermally-induced diffusion and dissolution of silver in spin-coated $As_{33}S_{67}$ amorphous films; their properties and structure. *J. Non-Cryst. Solids* **2003**, 326&327, 233-237.

[33] Wagner T.; Vlcek M.; Smrcina V.; Ewen P. J. S.; Owen A.E., Kinetics and reaction products of the photo-induced solid state chemical reaction between silver and amorphous $As_{33}S_{67}$ layers. *J. Non-Cryst. Solids* **1993**, 164-166, 1255-1258.

[34] Dutta N. S.; Arnold C. B., Scalable solution processing of amorphous and crystalline chalcogenide films *Trends Chem.* **2021**, 3, 535-546.

[35] Slang S.; Palka K.; Jain H.; Vlcek M., Influence of annealing on the optical properties, structure, photosensitivity and chemical stability of $As_{30}S_{70}$ spin-coated thin films. *J. Non-Cryst. Solids* **2017,** 457, 135-140.

[36] Slang S.; Palka K.; Loghina L.; Kovalskiy A.; Jain H.; Vlcek M., Mechanism of the dissolution of As–S chalcogenide glass in n-butylamine and its influence on the structure of spin coated layers. *J. Non-Cryst. Solids* **2015,** 426, 125-131.

[37] Kohoutek T.; Wagner T.; Frumar M.; Chrissanthopoulos A.; Kostadinova O.; Yannopoulos S. N., Effect of cluster size of chalcogenide glass nanocolloidal solutions on the surface morphology of spin-coated amorphous films. *J. Appl. Phys.* **2008**, 103, 063511.

[38] Messaddeq S. H.; Boily O.; Santagneli S. H.; El-Amraoui M.; Messaddeq Y., As_4S_4 role on the photoinduced birefringence of silver-doped chalcogenide thin films. *Opt. Mater. Express* **2016**, 6, 1451-1463.

[39] Stronski A.; Revutska L.; Meshalkin A.; Paiuk O.; Achimova E.; Korchovyi A.; Shportko K.; Gudymenko O.; Prisacar A.; Gubanova A.; Triduh G., Structural properties of Ag–As–S chalcogenide glasses in phase separation region and their application in holographic grating recording. *Opt. Mater.* **2019**, 94, 393-397.

[40] Cook J.; Slang S.; Golovchak R.; H. Jain; Vlcek M.; Kovalskiy A., Structural features of spin-coated thin films of binary As_xS_{100-x} chalcogenide glass system. *Thin Solid Films* **2015**, 589 642-648.

[41] Slang S.; Janicek P.; Palka K.; Loghina L.; Vlcek M., Optical properties and surface structuring of $Ge_{20}Sb_5S_{75}$ amorphous chalcogenide thin films deposited by spin-coating and vacuum thermal evaporation. *Mater. Chem. Phys.* **2018,** 203, 310-318.

[42] Golovchak R.; Shpotyuk O.; Mccloy J.S.; Riley B. J.; Windish C. F.; Sundaram S. K.; Kovalskiy A.; Jain H., Structural model of homogeneous As–S glasses derived from Raman spectroscopy and high-resolution XPS. *Philos Mag* **2010**, 90, 4489-4501.

[43] Pisarcik M.; Koudelka L., Raman spectra and structure of Ge-As-S glasses in the S-rich region. *Mater. Chem.* **1982**, 7, 499-508.

[44] Holomb R.; Mitsa V.; Petrachenkov O.; Veres M.; Stronski A.; Vlcek M., Comparison of structural transformations in bulk and as-evaporated optical media under action of polychromatic or photon-energy dependent monochromatic illumination. *Phys. Status Solidi C* **2011**, 8, 2705-2708.

[45] Musgraves J. D.; Wachtel P.; Gleason B.; Richardson K., Raman spectroscopic analysis of the Ge–As–S chalcogenide glass-forming system. *J. Non-Cryst. Solids* **2014**, 386, 61-66.

[46] Revutska L. O.; Shportko K. V.; Stronski A. V.; Baran J., Raman spectroscopy studies of Ge-As-S chalcogenide glasses. *2017 IEEE 7th International Conference Nanomaterials: Application & Properties (NAP)* **2017**, pp. 02NTF31-1-02NTF31-4.

[47] Slang S.; Palka K.; Vlcek M., Thermal dependence of photo-induced effects in spin-coated $As_{(20)}Ge_{(12.5)}S_{(67.5)}$ thin films. *J. Non-Cryst. Solids* **2017**, 471, 415-420.

[48] Jancalek J.; Slang S.; Kurka M.; Palka K.; Vlcek M., Preparation of quaternary solution processed chalcogenide thin films using mixtures of separate $As_{40}S_{60}$ and $Ge_{20}Sb_5S_{75}$ glass solutions. *J. Non-Cryst. Solids* **2021**, 564, 120833.

[49] Lin F.; Gulbiten O.; Yang Z.; Calvez L.; Lucas P., Mechanism of photostructural changes in mixed-chalcogen As–S–Se glasses investigated by Raman spectroscopy. *J. Phys. D. Appl. Phys.* **2011**, 44, 045404.

[50] Kohoutek T.; Wagner T.; Vlcek Mir.; Vlcek Mil.; Frumar M., Spin-coated $As_{33}S_{67-x}Se_x$ thin films: the effect of annealing on structure and optical properties. *J. Non-Cryst. Solids* **2006**, 352, 1563-1566.